A New Rare-Earth Indium Antimonide, (RE)$In_{1-x}Sb_2$ (RE = La−Nd), Featuring In Zigzag Chains and Sb Square Nets

Michael J. Ferguson, Robert E. Ellenwood, and Arthur Mar*

Department of Chemistry, University of Alberta, Edmonton, Alberta, Canada T6G 2G2

Received May 13, 1999

A new series of ternary rare-earth indium antimonides, (RE)$In_{1-x}Sb_2$ (RE = La−Nd), has been synthesized through reaction of the elements at 950 °C. The structure of $LaIn_{0.81(1)}Sb_2$ has been determined by single-crystal X-ray diffraction (monoclinic space group C_{2h}^2-$P2_1/m$, $Z = 2$, $a = 4.521(3)$ Å, $b = 4.331(3)$ Å, $c = 11.913(7)$ Å, $\beta = 99.6680(11)°$). The structure is built up of alternating layers of compositions $^2_\infty$[Sb] and $^2_\infty$[$In_{0.8}$Sb], separated by the La atoms. The $^2_\infty$[Sb] layer is described as a nearly square net of Sb atoms held by weak one-electron bonds, while the $^2_\infty$[$In_{0.8}$Sb] layer is derived from edge-sharing $InSb_4$ tetrahedra distorted in such a way as to produce In−In zigzag chains. Extended Hückel band structure calculations are used to explain the bonding and predict that anisotropic metallic behavior should be observed.

Introduction

The Zintl concept serves as a useful tool to interpret and understand the bonding in compounds of alkali or alkaline-earth metals and the elements of groups 13−16.[1−4] Within the concept, the electropositive elements serve to donate their valence electrons to the main-group elements, which use them to satisfy the octet rule, forming homoatomic bonds if necessary. This approximation can sometimes fail, particularly in cases where there are highly charged cations and small differences in electronegativities.

There exist a large number of ternary alkali- or alkaline-earth-metal main-group-element antimonides $A_xM_ySb_z$ (M = Al, Ga, In, Si, Ge, Sn), for which the Zintl concept works well in accounting for the structure of the anionic framework, which may contain both strong M−M and Sb−Sb bonds.[5] On the other hand, there are also many ternary rare-earth transition-metal antimonides $(RE)_xM_ySb_z$ (M = transition metal) for which the Zintl concept has to be extended to account for weak Sb−Sb bonds which often form a characteristic feature of these structures.[6] The latter compounds display a wide variety of electrical and magnetic behavior,[7−13] the most well-known being the promising thermoelectric properties of some filled skutterudites.[14]

Curiously, the only example of a ternary rare-earth main-group-element antimonide in the systems $(RE)_xM_ySb_z$ (M = Al, Ga, In, Si, Ge, Sn) is $LaSn_{0.75}Sb_2$.[15] We report here the structure of $LaIn_{0.8}Sb_2$, which is the first example of a rare-earth indium antimonide. Although both $LaSn_{0.75}Sb_2$ and $LaIn_{0.8}Sb_2$ are nonstoichiometric compounds, a wide homogeneity range is possible in $LaSn_xSb_2$ ($\sim 0.1 \le x \le \sim 0.8$) while $LaIn_{0.8}Sb_2$ is a point phase. The structures of $LaSn_{0.75}Sb_2$ and $LaIn_{0.8}Sb_2$ share some common features, notably the presence of weak Sb−Sb bonds in square sheets and strong Sn−Sn or In−In bonds in chains. We examine the nature of this bonding through extended Hückel band structure calculations.

Experimental Section

Synthesis. Starting materials were powders of the elements (La, Ce, Pr, Nd 99.9%, Alfa-Aesar; In 99.999%, Cerac; Sb 99.995%, Aldrich). The elements were loaded into fused-silica tubes (5 cm long, 10 mm i.d.) in a 1:0.8:2 ratio (total weight 250 mg). The tubes were then evacuated, sealed, and heated in a furnace at 570 °C for 1 day and at 950 °C for 2 days, cooled to 500 °C over 1 day, and finally cooled to room temperature over 5 h. The products were typically black powders interspersed with small plate-shaped crystals of the ternary compound. The crystal of $LaIn_{0.8}Sb_2$ analyzed by X-ray diffraction was selected from a reaction with a loaded stoichiometry of 1:1:2. Elemental compositions were obtained by EDX (energy-dispersive X-ray) analyses on a Hitachi F2700 scanning electron microscope, which indicated the presence of all three elements in a ratio consistent with the formula

(1) *Chemistry, Structure, and Bonding of Zintl Phases and Ions*; Kauzlarich, S. M., Ed.; VCH Publishers: New York, 1996.
(2) Schäfer, H. *Annu. Rev. Mater. Sci.* **1985**, *15*, 1.
(3) Corbett, J. D. *Chem. Rev.* **1985**, *85*, 383.
(4) von Schnering, H. G. *Angew. Chem., Int. Ed. Engl.* **1981**, *20*, 33.
(5) For example, see the following. (a) $Na_7Al_2Sb_5$: Cordier, G.; Ochmann, H.; Schäfer, H.; Stelter, M. *Z. Anorg. Allg. Chem.* **1984**, *517*, 118. (b) $Ca_5Ga_2Sb_6$, $Ca_5In_2Sb_6$, $Sr_5In_2Sb_6$: Cordier, G.; Schäfer, H.; Stelter, M. *Z. Naturforsch., B*: *Anorg. Chem., Org. Chem.* **1985**, *40*, 5. (c) $Na_2Ga_3Sb_3$: Cordier, G.; Ochmann, H.; Schäfer, H. *Mater. Res. Bull.* **1986**, *21*, 331. (d) $Ba_2Sn_3Sb_6$: Lam, R.; Mar, A. *Inorg. Chem.* **1996**, *21*, 6959. (e) Na_5SnSb_3, K_8SnSb_4: Eisenmann, B.; Klein, J. *Z. Naturforsch., B*: *Chem. Sci.* **1988**, *43*, 1156.
(6) For example, see the following. (a) La_3ZrSb_5, La_3HfSb_5, (RE)$CrSb_3$ (RE = La−Nd, Sm, Gd−Dy): Ferguson, M. J.; Hushagen, R. W.; Mar, A. *J. Alloys Compd.* **1997**, *249*, 191 and references therein. (b) (RE)$M_{1-x}Sb_2$ (RE = La−Nd, Sm, Gd, Tb; M = Mn, Co, Au, Zn, Cd): Wollesen, P.; Jeitschko, W.; Brylak, M.; Dietrich, L. *J. Alloys Compd.* **1996**, *245*, L5. (c) (RE)M_4Sb_{12} (RE = La−Nd, Sm, Eu; M = Fe, Ru, Os): Braun, D. J.; Jeitschko, W. *J. Less-Common Met.* **1980**, *72*, 147.
(7) Raju, N. P.; Greedan, J. E.; Ferguson, M. J.; Mar, A. *Chem. Mater.* **1998**, *10*, 3630.
(8) Hartjes, K.; Jeitschko, W.; Brylak, M. *J. Magn. Magn. Mater.* **1997**, *137*, 109.
(9) Muro, Y.; Takeda, N.; Ishikawa, M. *J. Alloys Compd.* **1997**, *257*, 23.
(10) André, G.; Bourée, F.; Oles, A.; Penc, B.; Sikora, W.; Szytula, A.; Zygmunt, A. *J. Alloys Compd.* **1997**, *255*, 31.
(11) Sologub, O.; Hiebl, K.; Rogl, P.; Bodak, O. *J. Alloys Compd.* **1995**, *227*, 40.
(12) Sologub, O.; Noël, H.; Leithe-Jasper, A.; Rogl, P.; Bodak, O. I. *J. Solid State Chem.* **1995**, *115*, 441.
(13) Sologub, O.; Hiebl, K.; Rogl, P.; Noël, H.; Bodak, O. *J. Alloys Compd.* **1994**, *210*, 153.
(14) Sales, B. C.; Mandrus, D.; Williams, P. K. *Science* **1996**, *272*, 1325.
(15) Ferguson, M. J.; Hushagen, R. W.; Mar, A. *Inorg. Chem.* **1996**, *35*, 4505.

10.1021/ic9905244 CCC: $18.00
Published on Web 09/16/1999

Table 1. Cell Parameters for Ternary (RE)$In_{0.8}Sb_2$ Compounds

compd	*a* (Å)	*b* (Å)	*c* (Å)	*β* (deg)	*V* (Å^3)
$LaIn_{0.8}Sb_2$	4.508(1)	4.350(1)	11.914(3)	99.41(1)	230.29(8)
$CeIn_{0.8}Sb_2$	4.478(2)	4.323(2)	11.796(5)	99.36(2)	225.2(1)
$PrIn_{0.8}Sb_2$	4.465(2)	4.303(2)	11.733(5)	99.45(2)	222.2(1)
$NdIn_{0.8}Sb_2$	4.445(4)	4.297(4)	11.677(9)	99.22(5)	220.1(2)

(RE)$In_{0.8}Sb_2$. Anal. Calcd (mol %): RE 26, In 21, Sb 53. Found (average of three analyses each): La 26.8(4), In 22(3), Sb 52(3); Ce 27.0(3), In 21(2), Sb 53(2); Pr 28.3(8), In 20(2), Sb 51.7(7). Since only powder was obtained for RE = Nd, EDX analysis was not performed on this member. Powder X-ray diffraction patterns were collected on an Enraf-Nonius FR552 Guinier camera (Si standard). The cell parameters were refined by least-squares fits of 28−42 reflections in the powder patterns with the program POLSQ[16] and are listed in Table 1. The observed powder X-ray diffraction patterns agree well with those calculated from the crystal structure of $LaIn_{0.8}Sb_2$ by the program LAZY-PULVERIX[17] (Tables S1−S4 (Supporting Information)).

Since the related $LaSn_xSb_2$ structure displays a wide homogeneity range ($\sim 0.1 \le x \le \sim 0.8$),[15] the potential for nonstoichiometric behavior of $LaIn_{0.8}Sb_2$ was investigated. Reactions performed as described above with loaded stoichiometry of $LaIn_xSb_2$ ($0.1 \le x \le 1.0$) were monitored by powder X-ray diffraction. The ternary phase could only be conclusively identified in reactions with $x \ge 0.6$, and from $x = \sim 0.8$ and higher, InSb formed along with the ternary compound. The products of the reactions with $x < 0.6$ could not be clearly identified but possibly contained $LaSb_2$ and other phases. In contrast to the nonstoichiometric behavior of $LaSn_xSb_2$, which was inferred by observing the shifting of the positions of reflections in the powder patterns,[15] the absence of such shifting for the $LaIn_xSb_2$ reactions suggests that $LaIn_{0.8}Sb_2$ either is a point phase or exists within a narrow range of composition. From the EDX analyses above, the other rare-earth members can be assumed to be substoichiometric in In as well. Redefining the subscript *x* to mean the deviation from full In occupancy, we refer to these compounds as "(RE)$In_{1-x}Sb_2$," where *x* is fixed at ~0.2.

Structure Determination. The thin plate-shaped crystals of $LaIn_{0.8}Sb_2$ are soft and highly prone to being bent, rendering them unsuitable for diffraction studies. After numerous crystals were screened for singularity by Weissenberg photography, a rather small (0.100 × 0.075 × 0.005 mm) crystal was finally selected. X-ray diffraction data were collected on two diffractometers, a Bruker P4/SMART CCD system and a Nonius Kappa CCD system. Both data sets led to the same structure solution and similar residuals in the final refinements, but as the Nonius data gave slightly better agreement with the EDX results and slightly better displacement parameters, these are the results reported. The data were collected at 293 K using a combination of ϕ rotations and ω scans. The frames were integrated using the Nonius maXus program, giving 2887 reflections, of which 563 were unique ($R_{int} = 0.045$). Final cell constants were determined using the HKL Scalepack program. Crystal data and further details of the data collection are given in Table 2 and in Table S5 and the CIF file (Supporting Information).

All calculations were carried out using the SHELXTL (Version 5.1) software package.[18,19] Conventional atomic scattering factors and anomalous dispersion corrections were used.[20] Intensity data were processed, and Gaussian face-indexed absorption corrections were applied with the program XPREP. The monoclinic space group $P2_1/m$ was selected on the basis of the intensity statistics, satisfactory averaging, and the successful structure solution. Although the monoclinic structure of $LaIn_{0.8}Sb_2$ is closely related to the orthorhombic structure of $LaSn_{0.75}Sb_2$, inspection of the reciprocal space plots shows the inequivalence of *hkl* and $\bar{h}kl$ reflections, and analysis of the final structure reveals no higher symmetry elements. The positions of all atoms were found by direct methods, and the structure was refined by least-squares methods. At this stage, an anomalously large displacement parameter for the In site suggested partial occupancy. Refinement of the occupancies of all atoms confirmed that the compound is substoichiometric only in In. The displacement parameters for all atoms were refined anisotropically. Although U_{eq} for In is larger than normal, we have confidence in the results because the resulting formula, $LaIn_{0.81(1)}Sb_2$, is consistent with that obtained from EDX analyses (vide supra). The large U_{eq} for In may be an artifact of the absorption correction, but given that the displacement parameters for the other atoms are well behaved, it is more likely that this is a real effect representing the tendency of the atoms "inserted" between the $LaSb_2$ layers to disorder over several sites, as has been observed in $LaSn_{0.75}Sb_2$.[15] The atomic positions were standardized with the use of the program STRUCTURE TIDY.[21] The final cycle of least-squares refinement on F_o^2 of 27 variables and 563 averaged reflections (including those having $F_o^2 < 0$) converged to values for $R_w(F_o^2)$ of 0.1308 and $R(F)$ (for $F_o^2 > 2\sigma(F_o^2)$) of 0.0491. The final difference electron density map is featureless ($\Delta\rho_{max} = 4.15$, $\Delta\rho_{min} = -2.92$ e Å^{-3}). Final values of the positional and equivalent isotropic displacement parameters are given in Table 3, anisotropic displacement parameters are given in Table S6, and final structure amplitudes are available from A.M.

Table 2. Crystallographic Data for $LaIn_{0.8}Sb_2$

empirical formula: $LaIn_{0.8}Sb_2$	$C_{2h}^2-P2_1/m$ (No. 11)
fw 474.27	$T = 20$ °C
$a = 4.521(3)$ Å[a]	$\lambda = 0.710\ 73$ Å
$b = 4.331(3)$ Å[a]	$\rho_{calc} = 6.850$ g cm^{-3}
$c = 11.913(7)$ Å[a]	$\mu = 244.80$ cm^{-1}
$\beta = 99.6680(11)°$	$R(F)$ for $F_o^2 > 2\sigma(F_o^2)$[b] $= 0.0491$
$V = 229.9(2)$ Å^3	$R_w(F_o^2)$[c] $= 0.1308$
$Z = 2$	

[a] Obtained from refinement constrained so that $\alpha = \gamma = 90°$. [b] $R(F) = \Sigma||F_o| - |F_c||/\Sigma|F_o|$. [c] $R_w(F_o^2) = [\Sigma w(F_o^2 - F_c^2)^2/\Sigma wF_o^4]^{1/2}$; $w^{-1} = [\sigma^2(F_o^2) + (0.0344p)^2 + 32.59p]$, where $p = [\max(F_o^2, 0) + 2F_c^2]/3$.

Table 3. Atomic Coordinates, Occupancies, and Equivalent Isotropic Displacement Parameters (Å^2) for $LaIn_{0.8}Sb_2$

atom	Wyckoff position	*x*	*y*	*z*	occupancy	U_{eq}[a]
La	2*e*	0.8440(4)	1/4	0.2160(1)	1	0.0097(5)
In	2*e*	0.2139(8)	1/4	0.4846(2)	0.81(1)	0.0341(12)
Sb(1)	2*e*	0.6158(4)	1/4	0.6951(2)	1	0.0107(5)
Sb(2)	2*e*	0.2489(4)	1/4	0.0016(2)	1	0.0101(5)

[a] U_{eq} is defined as one-third of the trace of the orthogonalized $\mathbf{U}_{ij}$ tensor.

Band Structure. One-electron band structure calculations on a hypothetical fully occupied $LaInSb_2$ structure as well as a 1 × 2 × 1 superstructure model were performed by the tight-binding method with an extended Hückel-type Hamiltonian using the EHMACC suite of programs.[22,23] The atomic parameters used are listed in Table 4.[24−26] Properties were extracted from the band structure using 192 k points in the irreducible portion of the Brillouin zone.

Results and Discussion

Description of the Structure. A view of the structure down the *b* axis is shown in Figure 1a, which also shows the labeling

(16) POLSQ: Program for least-squares unit cell refinement. Modified by D. Cahen and D. Keszler, Northwestern University, 1983.
(17) Yvon, K.; Jeitschko, W.; Parthé, E. *J. Appl. Crystallogr.* **1977**, *10*, 73.
(18) Sheldrick, G. M. *SHELXTL*, Version 5.1; Bruker Analytical X-ray Systems, Inc.: Madison, WI, 1997.
(19) Sheldrick, G. M. *J. Appl. Crystallogr.*, in press.
(20) *International Tables for X-ray Crystallography*; Wilson, A. J. C., Ed.; Kluwer: Dordrecht, The Netherlands, 1992; Vol. C.
(21) Gelato, L. M.; Parthé, E. *J. Appl. Crystallogr.* **1987**, *20*, 139.
(22) Whangbo, M.-H.; Hoffmann, R. *J. Am. Chem. Soc.* **1978**, *100*, 6093.
(23) Hoffmann, R. *Solids and Surfaces*: *A Chemist's View of Bonding in Extended Structures*; VCH Publishers: New York, 1988.
(24) Lulei, M.; Martin, J. D.; Hoistad, L. M.; Corbett, J. D. *J. Am. Chem. Soc.* **1997**, *119*, 513.
(25) Canadell, E.; Eisenstein, O.; Rubio, J. *Organometallics* **1984**, *3*, 759.
(26) Hughbanks, T.; Hoffmann, R.; Whangbo, M.-H.; Stewart, K. R.; Eisenstein, O.; Canadell, E. *J. Am. Chem. Soc.* **1982**, *104*, 3876.

Table 4. Extended Hückel Parameters

atom	orbital	H_{ii} (eV)	ζ_{i1}	c_1	ζ_{i2}	c_2
La	6s	−6.5613	2.14			
	6p	−4.3769	2.08			
	5d	−7.5155	3.78	0.776 51	1.381	0.458 61
In	5s	−12.60	1.903			
	5p	−6.19	1.677			
Sb	5s	−18.8	2.323			
	5p	−11.7	1.999			

Table 5. Selected Interatomic Distances (Å) and Angles (deg) for $LaIn_{0.8}Sb_2$

La−Sb(1)	3.297(2) (2×)	In−Sb(1)	2.839(3)
La−Sb(1)	3.303(2) (2×)	In−Sb(1)	3.228(3) (2×)
La−Sb(2)	3.349(2) (2×)	In−In	2.967(5) (2×)
La−Sb(2)	3.384(3)	In−In	3.346(6) (2×)
La−Sb(2)	3.385(3)	Sb(2)−Sb(2)	3.119(3) (2×)
La−In	3.352(4)	Sb(2)−Sb(2)	3.142(3) (2×)

Sb(1)−La−Sb(1)	82.11(7)	Sb(1)−La−In	86.21(7)
Sb(1)−La−Sb(1)	143.11(8)	Sb(1)−La−In	58.02(5)
Sb(1)−La−Sb(1)	86.48(5)	Sb(2)−La−In	135.75(5)
Sb(1)−La−Sb(1)	81.94(7)		
Sb(1)−La−Sb(2)	79.63(5)	In−In−In	93.7(2)
Sb(1)−La−Sb(2)	132.01(7)	Sb(1)−In−Sb(1)	84.27(10)
Sb(1)−La−Sb(2)	131.45(6)	In−In−Sb(1)	79.95(8)
Sb(1)−La−Sb(2)	79.29(5)	In−In−Sb(1)	143.59(16)
Sb(1)−La−Sb(2)	133.85(4)	Sb(1)−In−Sb(1)	113.41(10)
Sb(1)−La−Sb(2)	77.13(6)	Sb(1)−In−In	103.93(16)
Sb(1)−La−Sb(2)	77.20(6)		
Sb(1)−La−Sb(2)	133.89(4)	Sb(2)−Sb(2)−Sb(2)	87.93(10)
Sb(2)−La−Sb(2)	80.56(7)	Sb(2)−Sb(2)−Sb(2)	178.61(12)
Sb(2)−La−Sb(2)	55.19(5)	Sb(2)−Sb(2)−Sb(2)	92.45(5)
Sb(2)−La−Sb(2)	55.62(5)	Sb(2)−Sb(2)−Sb(2)	87.13(10)
Sb(2)−La−Sb(2)	83.82(7)		

scheme. Selected interatomic distances and angles are given in Table 5. The structure consists of layers of compositions $^2_\infty$[Sb] and $^2_\infty$[$In_{0.8}Sb$] stacked parallel to the 001 plane, separated by La atoms. A perpendicular view of the structure down the *a* axis is shown in Figure 1b. The La atoms are coordinated by eight Sb atoms in a square antiprismatic fashion, as shown in Figure 2a. Four Sb(1) atoms define one square of Sb atoms, and four Sb(2) atoms define the second square, which is twisted 45° relative to the first. A ninth capping atom of In is situated above the larger square of Sb(1) atoms and is tilted to one side. The Sb(2) atoms are surrounded by four other symmetry-equivalent Sb(2) atoms, forming a nearly flat square sheet, $^2_\infty$[Sb]. The La atoms are positioned above and below this sheet in an alternating "checkerboard" fashion. The In atoms are coordinated by three Sb(1) atoms and two In atoms in a distorted square pyramidal fashion, as shown in Figure 2b. The base of the pyramid is defined by two Sb(1) atoms and two In atoms, while the apical site is the third Sb(1) atom. These square pyramidal units are condensed via corner-sharing of the basal atoms along [010] to form zigzag In chains (Figure 1) and coupled in a head-to-tail fashion along [100] to form the infinite sheet $^2_\infty$[$In_{0.8}Sb$].

Structural Relationships. The coordination environment around rare-earth metal atoms in solid-state compounds is flexible (typically CN 8 or 9) and is strongly influenced by the bonding requirements of the more electronegative components. The RE atoms are commonly found with square antiprismatic coordination by Sb in structures that feature Sb square nets, as observed in (RE)M_xSb_2 (M = Mn − Zn, Pd, Ag, Cd, Au),[6b] and sometimes have a ninth capping Sb atom, as observed in (RE)Sb_2[27,28] and (RE)MSb_3 (M = V, Cr).[6a,29] The La−Sb bond lengths in $LaIn_{0.8}Sb_2$ that define the square antiprism are within the range of interatomic distances found in these compounds (3.29−3.39 Å).[6a,b,15] The ninth capping atom is In instead of Sb, at a distance of 3.352(4) Å, within the range found in binary lanthanum indides (3.168−3.721 Å).[30]

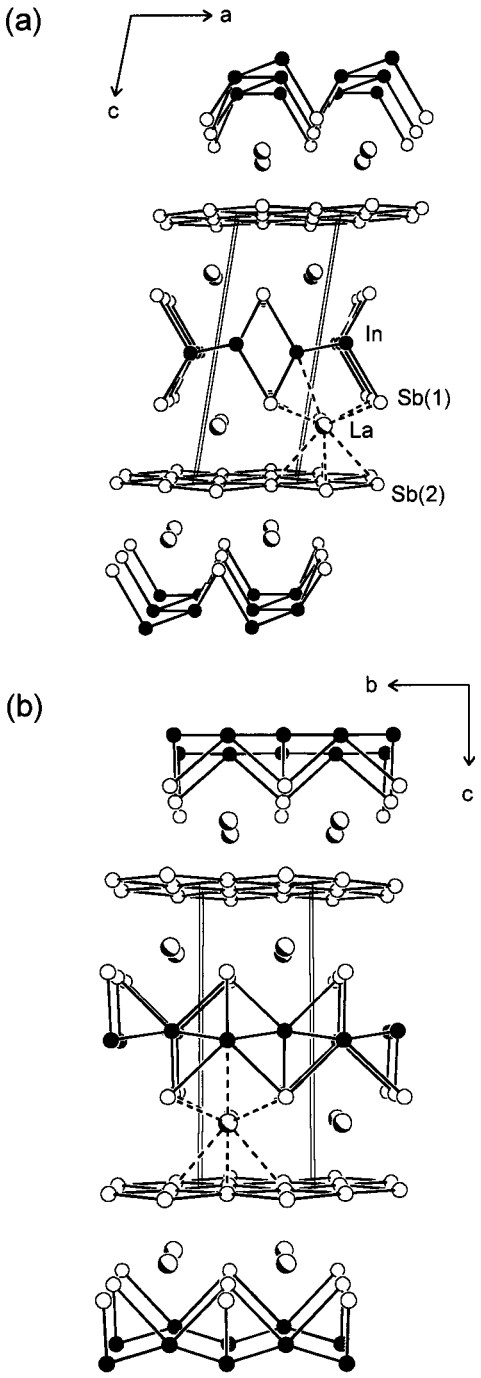

Figure 1. (a) View down the *b* axis of $LaIn_{0.8}Sb_2$ with the unit cell outlined, showing the zigzag In chains and square nets of Sb. The partly shaded circles are La atoms, the solid circles are In atoms, and the open circles are Sb atoms. (b) View of the structure down the *a* axis.

A natural choice of structures in which to examine relationships is the series $LaM_{1-x}Sb_2$, where M = Cd, In, and Sn. All contain layers of $^2_\infty$[$LaSb_2$] composed of Sb square sheets and square antiprismatic coordination of La, separated by layers

(27) Wang, R.; Steinfink, H. *Inorg. Chem.* **1967**, *6*, 1685.

(28) Eatough, N. L.; Hall, H. T. *Inorg. Chem.* **1969**, *8*, 1439.

(29) Brylak, M.; Jeitschko, W. *Z. Naturforsch., B*: *Chem. Sci.* **1995**, *50*, 899.

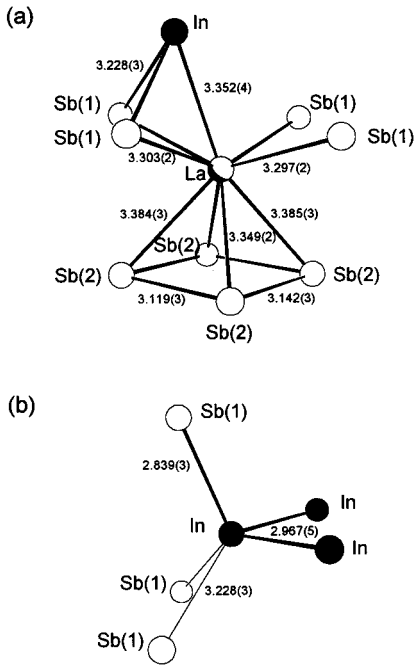

Figure 2. (a) Coordination of the La atom by eight Sb atoms in a square antiprismatic fashion, capped by an In atom, with the La−Sb, La−In, and Sb(2)−Sb(2) bond lengths indicated. (b) Distorted square pyramidal coordination around the In atom, with the In−In and In−Sb(1) bond lengths shown.

of the M atoms, as shown in Figure 3. The three closely related structures differ in the nature of these M layers. In the structure of $LaCd_{0.7}Sb_2$ ($HfCuSi_2$-type), the Cd atoms form a perfectly square sheet with Cd−Cd distances of 3.111(2) Å.[6b] When this is compared to the 3.02 Å distance found in elemental Cd,[31] it is tempting to suggest a weak $d^{10}-d^{10}$ bonding interaction in $LaCd_{0.7}Sb_2$. The In layer in $LaIn_{0.8}Sb_2$ can be viewed as a distortion of a square net to form parallel zigzag chains, with intra- and interchain In−In distances of 2.967(5) and 3.346(6) Å, respectively. Zigzag chains with similar In−In intrachain distances are observed in the binary compound Li_2In (In−In distance 2.926 Å),[32] and significantly longer distances are observed in the ternary compounds $(AE)_4In_2N$ (In−In distance: 3.162 Å when AE = Ca; 3.320 Å when AE = Sr).[33] Since even longer distances of 3.24 and 3.36 Å are found in the structure of elemental In,[31] it will be important to quantify the degree of In−In bonding in $LaIn_{0.8}Sb_2$ to decide if the description of In zigzag chains or a distorted square net is more appropriate. As we demonstrate later from the results of the band structure calculations, the zigzag chains are an integral part of this structure. Finally, the structure of $LaSn_{0.75}Sb_2$ represents an extreme in this distortion process, resulting in an Sn layer that consists of linear chains partially occupied in a disordered fashion and Sn−Sn distances of 2.814−2.844 Å on a local level.[15]

The Sb square nets also undergo slight distortions from the perfectly square net found in $LaCd_{0.7}Sb_2$ (Sb−Sb distance 3.111 Å; angles 90, 180°)[6b] to the nets observed in $LaIn_{0.8}Sb_2$ (Sb−Sb distances 3.119 (2×), 3.142 Å (2×); angles 87.13, 87.93, 92.45, 178.61°) and $LaSn_{0.75}Sb_2$ (Sb−Sb distance 3.0952 Å; angles 86.55, 93.40, 177.60°).[15] Since these bond lengths are similar, it is reasonable to assume that the Sb−Sb bond strength in each net is also similar. The distortion from a perfect square Sb net is driven by the nature of the bonding in the M layer and is reflected in the changing of the symmetry from tetragonal to monoclinic to orthorhombic; the geometry of the Sb net must change as well.

It is important to note that, in Figure 3, the M layers were drawn without any M−Sb bonds shown to allow for easier comparison, but obviously they cannot be neglected. Several alkali- and alkaline-earth-metal indium antimonides are known with structures that are based on different connectivities of $InSb_4$ tetrahedral units, although none display In−In bonding.[5b,34] It is more instructive to view the $In_{0.8}Sb$ layer in $LaIn_{0.8}Sb_2$ as a distortion of the $Cd_{0.7}Sb$ layer in $LaCd_{0.7}Sb_2$ (Figure 4). Antimony atoms reside above and below the centers of the Cd squares in an alternating "checkerboard" pattern. Each Cd is tetrahedrally coordinated by four Sb atoms, with bond lengths of 2.898 Å.[6b] The distortion of the In layer to zigzag chains is accompanied by a slight canting of the chains, such that they are no longer coplanar (Figure 1). The position of the Sb atom is shifted off-center and bonds to three In atoms inequivalently (In−Sb distances 2.839 and 3.228 Å (2×)). The shorter distance is typical of the In−Sb single bonds observed in $InSb_4$ tetrahedra (2.804−3.100 Å)[35] found in ternary alkali- and alkaline-earth-metal indium antimonides and corresponds to the sum of the covalent radii (In, 1.44 Å; Sb, 1.36 Å).[36]

Bonding and Band Structure. As a first approximation, oxidation states can be assigned on the basis of the Zintl concept. By considering the electronegativities of the three elements (Pauling: La, 1.10; In, 1.78; Sb, 2.05),[37] we can assume that the La atoms transfer their electrons to the In and Sb atoms, which use them to form bonds and complete their octets. We first consider the hypothetical, fully occupied structure, $LaInSb_2$, and then examine the effect of In substoichiometry. The structure naturally partitions into two anionic layers of Sb(2) and InSb(1) separated by La cations as represented by $(La^{3+})[(InSb(1))(Sb(2))]^{3-}$. The Sb(2)−Sb(2) bond lengths (∼3.1 Å) are intermediate between the intralayer, single-bond length and the weakly bonding interlayer distance observed in elemental Sb (2.908 and 3.36 Å, respectively).[31] These ∼3.1 Å interactions have been successfully modeled as half-bonds (or one-electron bonds), and the Sb atoms have been assigned an oxidation state of −1.[29,38] Each Sb(2) atom has two lone pairs of electrons in the 5s and $5p_z$ orbitals or some hybridized equivalent and bonds through the $5p_x$ and $5p_y$ orbitals to form the square net. The

(30) La_3In: 3.596 Å. La_2In: 3.251−3.704 Å. La_3In_5: 3.168−3.639 Å. $LaIn_2$: 3.378−3.721 Å. $LaIn_3$: 3.348 Å. McMasters, O. D.; Gschneidner, K. A., Jr. *J. Less-Common Met.* **1974**, *38*, 137 and references therein.
(31) Greenwood, N. N.; Earnshaw, A. *Chemistry of the Elements*; Pergamon Press: Oxford, U.K., 1994.
(32) Stöhr, J.; Müller, W.; Schäfer, H. *Z. Naturforsch., B*: *Anorg. Chem., Org. Chem.* **1978**, *33*, 1434.
(33) Cordier, G.; Rönninger, S. *Z. Naturforsch., B*: *Chem. Sci.* **1987**, *42*, 825.
(34) (a) $Na_2In_2Sb_3$: Cordier, G.; Ochmann, H. *Z. Kristallogr.* **1991**, *197*, 281. (b) $K_2In_2Sb_3$: Cordier, G.; Ochmann, H. *Z. Kristallogr.* **1991**, *197*, 291. (c) $Rb_2In_2Sb_3$: Gourdon, O.; Boucher, F.; Gareh, J.; Evain, M.; O'Connor, C. J.; Jin-Seung, J. *Acta Crystallogr., Sect C*: *Cryst. Struct. Commun.* **1996**, *52*, 2963. (d) $Cs_2In_2Sb_3$: Blase, W.; Cordier, G.; Poth, L.; Weil, K. G. *Z. Kristallogr.* **1995**, *210*, 60. (e) $Ba_5In_2Sb_6$: Cordier, G.; Stelter, M. *Z. Naturforsch., B*: *Chem. Sci.* **1988**, *43*, 463. (f) Na_3InSb_2: Cordier, G.; Ochmann, H. *Z. Kristallogr.* **1991**, *195*, 107. (g) $Ca_{11}InSb_9$: Cordier, G.; Schäfer, H.; Stelter, M. *Z. Naturforsch., B*: *Anorg. Chem., Org. Chem.* **1985**, *40*, 868.
(35) In−Sb distances: $Cs_2In_2Sb_3$, 2.804−2.962 Å;[34d] $Ba_5In_2Sb_6$, 2.853−3.100 Å;[34e] Na_3InSb_2, 2.846−2.962 Å;[34f] $Ca_{11}InSb_9$, 2.881−2.886 Å.[34g]
(36) Pauling, L. *The Nature of the Chemical Bond*, 3rd ed.; Cornell University Press: Ithaca, NY, 1960.
(37) Cotton, F. A.; Wilkinson, G. *Advanced Inorganic Chemistry*, 3rd ed.; John Wiley & Sons: New York, 1972.
(38) Brylak, M.; Jeitschko, W. *Z. Naturforsch., B*: *Chem. Sci.* **1994**, *49*, 747.

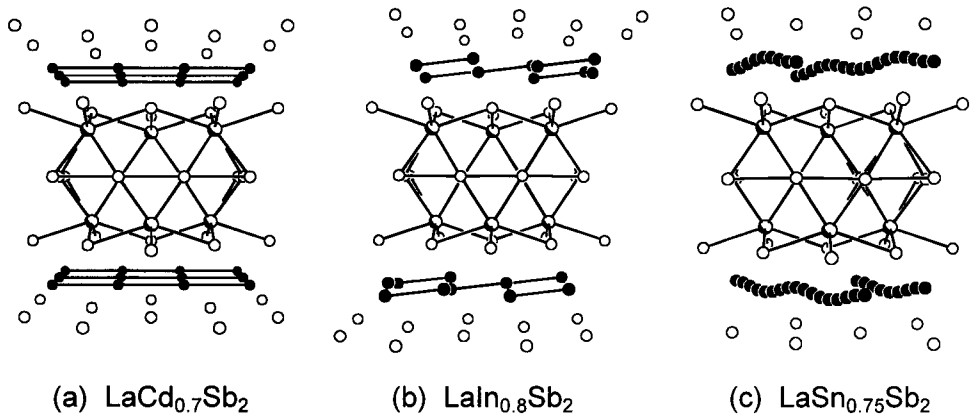

Figure 3. Comparison of the layered $(RE)_xM_ySb_z$ structures: (a) $LaCd_{0.7}Sb_2$, a member of the $(RE)MSb_2$ (M = Mn−Zn, Pd, Ag, Cd, Au) series; (b) $LaIn_{0.8}Sb_2$; (c) $LaSn_{0.75}Sb_2$. The partly shaded circles are the La atoms, the solid circles are the M atoms (Cd, In, or Sn), and the open circles are Sb atoms. The perfectly square M layer in $LaCd_{0.7}Sb_2$ distorts into zigzag chains in $LaIn_{0.8}Sb_2$, and finally to disordered linear chains in $LaSn_{0.75}Sb_2$.

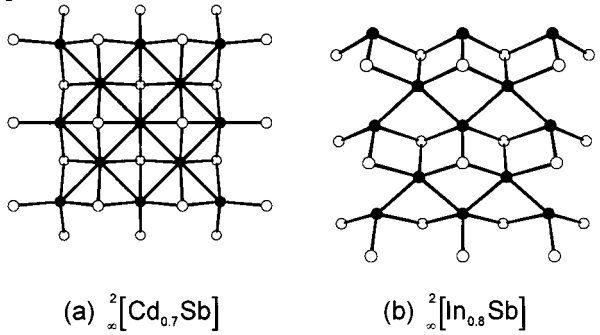

Figure 4. Comparison of the ideal square MSb layer in $LaCd_{0.7}Sb_2$ to the distorted layer in $LaIn_{0.8}Sb_2$. Note that the Sb atoms no longer reside in the center of M squares in $LaIn_{0.8}Sb_2$.

nearest Sb(1)−Sb(1) interactions are greater than 4.3 Å, approximately equal to the sum of the van der Waals radii (∼2.2 Å),[36] and are therefore considered as isolated $Sb(1)^{3-}$ anions. Charge balance requires that the In atoms have an oxidation state of +1, resulting in an overall formulation of $[(La^{3+})(In^{+})(Sb(1)^{3-})(Sb(2)^{-})]$. Although this seems to imply the presence of a lone pair of electrons on In, these electrons are used to form the In−In zigzag chains. Using three sp^3 hybrid orbitals, each In makes two single bonds to neighboring In atoms (2.967 Å) and one single bond to an Sb(1) atom (2.839 Å). The fourth sp^3 hybrid orbital is involved in forming two longer In−Sb bonds (3.228 Å), which can be viewed together as a 3-center−2-electron bond (i.e., each is a one-electron bond) consistent with the weaker and longer interaction.

But the actual formula is substoichiometric in In content, which reduces the valence electron count (vec) from 16 to 15.4 per formula unit and necessitates a modification of the oxidation state assignments. The easiest solution is to assign a fractional oxidation state to In to yield $[(La^{3+})(In^{1.25+})_{0.8}(Sb(1)^{3-})(Sb(2)^{-})]$ and assume that the rest of the atoms are unchanged. This would correspond to a weakening of the bonding in the zigzag chains, while not altering the Sb bonding in the square net. A second possibility could be the oxidation of the Sb(2) square net, since such nets have been previously postulated to serve as electron "sources" or "sinks".[6a] A combination of both oxidation processes could occur, of course. The question that arises is thus whether there is some underlying electronic reason that requires the In content to be substoichiometric. To attempt to answer this, and to test the validity of the bonding model proposed above, extended Hückel band structure calculations were performed.

Partial occupancy can be problematic to handle in the extended Hückel method. To address this, two models were considered: (1) a stoichiometric $LaInSb_2$, with the In deficiencies in $LaIn_{0.81(1)}Sb_2$ modeled by lowering the vec from 16 to 15.4, and (2) a $1 \times 2 \times 1$ superstructure (i.e., the unit cell is doubled along *b*) with every fourth In atom removed along the zigzag chain, corresponding to the formula $LaIn_{0.75}Sb_2$, which approximates the real formula of $LaIn_{0.81(1)}Sb_2$. The results obtained from calculations on these two models are similar, and while we discuss both, we only show plots for the first model.

Starting with the first model of a substoichiometric $LaIn_{0.8}Sb_2$ produced by lowering the vec and following a "retrotheoretical analysis"[39] (whereby the complete structure is dissected into more manageable subunits to aid in interpretation and then reassembled for the complete picture), we arrive at the same partitioning described earlier. Removal of the La cations leaves anionic layers of Sb^- and $In_{0.8}Sb^{2-}$, which are sufficiently well separated and noninteracting, and the band structure of the anionic framework $[In_{0.8}Sb_2]^{3-}$ is simply a superposition of the band structures of each layer. Incorporation of the La cations does not drastically alter the overall nature of the band structure. Shown in Figure 5a is the density of states (DOS) curve for $LaIn_{0.8}Sb_2$, with the Fermi level ($\epsilon_f = -8.65$ eV) corresponding to the substoichiometric formula indicated. The individual atomic contributions to the DOS are plotted in Figure 5b−d. Although most of the La states are located above −7 eV, they make a significant contribution below ϵ_f, implying there is some degree of covalent character in the La−Sb and La−In bonds. The Fermi level crosses a small peak in the DOS and metallic behavior is expected.

The band dispersion plots along the special symmetry lines ΓX, ΓY (coplanar with the In chains), and ΓZ (parallel to the stacking axis) are shown in Figure 6. The Fermi level crosses two bands along ΓX, with orbital contributions from both the $In_{0.8}Sb$ layer and the Sb net, as well as some contribution from La states. Along ΓY, the Fermi level crosses only one band composed of Sb and La states. Although the In zigzag chains are randomly segmented by the vacancies, these segments are still cross-linked together by Sb(1) atoms, providing a pathway through which conduction can occur. Bands originating from the Sb(2) net are also crossed by the Fermi level and provide an additional pathway for conduction. Since there are no bands crossed along ΓZ, $LaIn_{0.8}Sb_2$ is predicted to be an anisotropic metal: conducting within the layers and insulating between.

(39) Papoian, G.; Hoffmann, R. *J. Solid State Chem.* **1998**, *139*, 8.

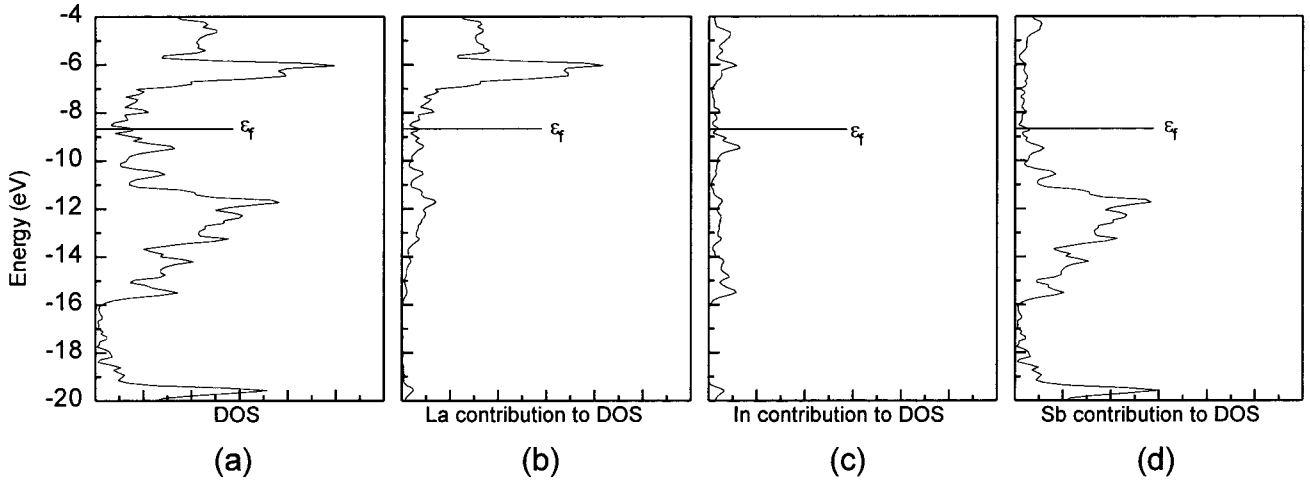

Figure 5. (a) Total density of states for $LaIn_{0.8}Sb_2$. The individual atomic contributions (La, In, and Sb) to the density of states are shown in (b)−(d). The Fermi level corresponding to the substoichiometric $LaIn_{0.8}Sb_2$ is shown.

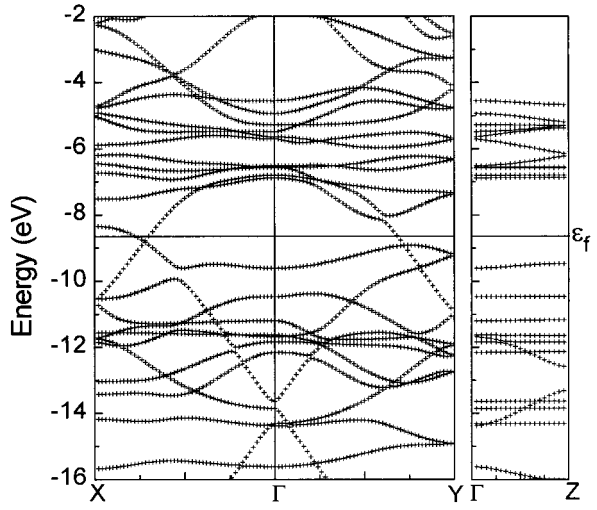

Figure 6. Band dispersion curves for $LaIn_{0.8}Sb_2$ along the special symmetry lines ΓX, ΓY, and ΓZ. The Fermi level corresponding to the substoichiometric $LaIn_{0.8}Sb_2$ is shown.

(The small dimensions of $LaIn_{0.8}Sb_2$ crystals have thus far precluded us from carrying out resistivity measurements.)

The nature of the bonding is best examined through the crystal orbital overlap population (COOP) curves, plotted in Figure 7, for the In−In, In−Sb, and Sb−Sb contacts. Clearly, the representation of In−In-bonded zigzag chains (instead of a distorted square net with each In atom forming four homoatomic bonds) is correct since only the shorter intrachain distance of 2.967 Å has significant bonding character (considerable filling of bonding states), while at the longer interchain distance of 3.346 Å, there are negligible interactions. On a local level, the 80% occupancy of In sites can be modeled as an infinite chain with every fifth site vacant, as shown in Figure 8. (This is one possibility of an ordered superstructure; in the actual structure, we assume that the chain is segmented randomly.) In a five-membered segment, the effect of one vacancy is to eliminate two of the five possible bonds, and therefore each In atom on average has only 60% of the maximum of two bonds (i.e., 1.2 bonds each). This gives an overlap population per bond of 0.65, which is comparable to that calculated for In−In single bonds in $BaIn_2$ (distance 3.03 Å, overlap population ∼0.64−0.76)[40] and for the 1-D linear In^+ chains (distance 2.90, overlap population 0.69)[41] found in $InMo_4O_6$.[42] In contrast, the overlap population for the longer In−In interchain distance (3.346 Å) is only ∼0.05, confirming the zigzag chain representation. The short In−Sb contact maximizes its bonding at the Fermi level, with an overlap population of 0.69, corresponding to a full single bond, while the longer In−Sb contact corresponds to a significant amount of antibonding states being filled (overlap population 0.28), roughly corresponding to a half-bond. Finally, the Sb−Sb bonding in the square net is exactly as expected, with some antibonding states filled and an overlap population (0.27) consistent with half-bonds. The La−Sb and La−In bonds have overlap populations consistent with some degree of covalency (0.24 and 0.16, respectively), which is not unexpected as a fully charged La^{3+} would strongly polarize the electron clouds of both the In and Sb atoms. The calculated atomic charges result in a formulation of $(La^{0.85+})(In^{0.45+})_{0.8}(Sb(1)^-)(Sb(2)^{0.2-})$. Considering that covalency will reduce extreme charges as required by the electroneutrality principle, these charges are in good agreement with the relative charges predicted by the Zintl concept.

The second model (an ordered $1 \times 2 \times 1$ superstructure with unit cell contents "$La_4In_3Sb_8$" or a formula $LaIn_{0.75}Sb_2$ with $Z = 4$) gave results that are generally consistent with those of the first model. In this case, every fourth In atom was removed in an ordered fashion along *b*, segmenting the infinite zigzag chains into finite three-membered units. The DOS curve and their individual atomic contributions, band dispersion, and COOP curves are given in the Supporting Information (Figures S1−S3). As before, the Fermi level ($\epsilon_f = -8.06$ eV) crosses a small peak in the DOS, with two bands being crossed along ΓX, one band along ΓY, and none along ΓZ; the picture of an anisotropic metal is still valid. There are slight differences in the values of the overlap population per bond, with the largest effect noted for the In−In intrachain (2.967 Å) interaction, which decreases from 0.65 (model 1) to 0.48 (model 2). This remains a strongly bonding interaction, especially when compared to the negligible interchain overlap population of 0.03 (model 2). Finally, the calculated atomic charges from the second model yield $(La^{0.75+})(In^{0.88+})_{0.75}(Sb(1)^{1.16-})(Sb(2)^{0.25-})$. The greater positive charge on In versus La can be explained by noting that the orbital energy for the La 5d states is lower than that of the

(40) Nuspl, G.; Polborn, K.; Evers, J.; Landrum, G. A.; Hoffmann, R. *Inorg. Chem.* **1996**, *35*, 6922.

(41) Janiak, C.; Hoffmann, R. *J. Am. Chem. Soc.* **1990**, *112*, 5924.

(42) McCarley, R. E.; Lii, K.-H.; Edwards, P. A.; Brough, L. F. *J. Solid State Chem.* **1985**, *57*, 17.

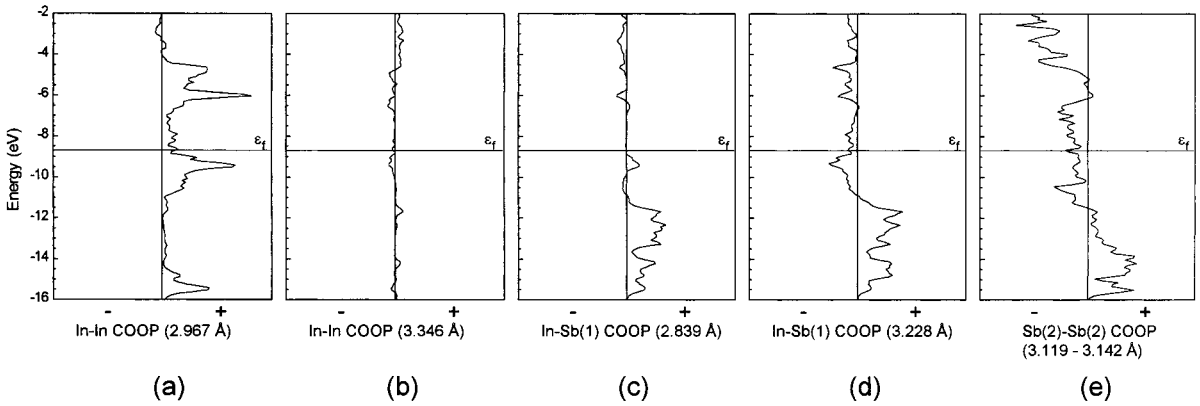

Figure 7. Crystal orbital overlap population curves for the In−In ((a) 2.967 and (b) 3.346 Å), In−Sb(1) ((c) 2.839 and (d) 3.228 Å), and Sb(2)−Sb(2) (e) interactions. The Fermi level corresponding to the substoichiometric $LaIn_{0.8}Sb_2$ is shown.

Figure 8. View of an ordered In chain with every fifth site vacant, as indicated by the dotted hollow circles. Removal of *one* In atom per five-membered segment removes *two* of the five possible In−In bonds.

In 5p states (Table 4) and that the 5d states are therefore likely to be more highly populated.

In conclusion, we have shown that $LaIn_{0.8}Sb_2$ provides an interesting example of how strong bonding between the heavier main-group elements (In−In) can coexist with weaker bonding (Sb−Sb). In particular, substoichiometry of the In sites seems to be necessary to provide a balance between the locally maximized In−In bonding within the zigzag chains and the weak Sb−Sb bonding within the square net. Although the immediate effect of increasing the number of electrons would be to slightly increase the strength of the In−In bonding, this would be strongly offset by the dramatic weakening of the Sb−Sb bonding, so the Sb square net remains intact in the real structure. This provides a clue to the origins of the substantial range of homogeneity observed for the corresponding $LaSn_x$-Sb_2 ($0.1 < x < 0.8$) system on one hand and the point phase nature of $LaIn_{0.8}Sb_2$ on the other. Replacing In with Sn puts more electrons into the system, which can be absorbed by the Sb square net to only a certain degree before other bonds (the Sn−Sn bonds in the $^2_\infty[Sn_xSb]$ layer) must break. This occurs, not by substantial lengthening of Sn−Sn bonds but rather by creation of vacancies to retain strong Sn−Sn bonds on a local level. It would be interesting, then, to explore the quaternary $LaIn_xSn_ySb_2$ system, and preliminary results suggest that such phases can be prepared.[43]

Acknowledgment. Financial support from the Natural Sciences and Engineering Research Council of Canada is gratefully acknowledged. We thank Daniel Frankel (Nonius Co., Bohemia, NY), Scott Lovell (Department of Chemistry, University of Washington, Seattle, WA), and Charles F. Campana (Bruker Analytical X-ray Systems, Inc., Madison, WI) for the collection of the X-ray data sets and assistance in the structure solution.

Supporting Information Available: Listings of powder X-ray diffraction data for $(RE)In_{0.8}Sb_2$ (RE = La−Nd), further crystallographic details, anisotropic displacement parameters, and additional interatomic distances and angles, plots from the band structure calculations on the superstructure $LaIn_{0.75}Sb_2$ (DOS with individual atomic contributions, band dispersion, and COOP curves), and an X-ray crystallographic file in CIF format. This material is available free of charge via the Internet at http://pubs.acs.org.

IC9905244

(43) Ellenwood, R. E.; Eulert, J. A.; Mar, A. Unpublished results.